JOURNAL OF MATERIALS SCIENCE 17 (1982) 2825–2830

Indentation study of cadmium oxalate trihydrate single crystals

S. K. ARORA, TOMY ABRAHAM, G. S. TRIVIKRAMA RAO, R. S. GODBOLE
Department of Physics, Sardar Patel University, Vallabh Vidyanagar 388 120, Gujarat, India

Vickers microhardness indentation studies have been made on the as-grown ($\bar{2}\bar{2}1$), (110) and (001) planes, and on the only cleavage plane ($1\bar{1}0$) of gel-grown cadmium oxalate trihydrate single crystals. The material chipping off and slip lines observed around indentation figures have been discussed. The anisotropy in microhardness of the crystals is indicated.

1. Introduction

Point indintation techniques, long used as a basis for routine hardness testing (e.g. Vickers pyramid test, Knoop test), are finding increasing application in the study of mechanical properties of brittle solids. Buckle [1, 2] has pointed out the possibility of investigating various material properties by means of microhardness measurements. Indentation is generally carried out using sharp indenters such as cones or pyramids because of the geometrical similarity of the residual impression; the contact pressure with such geometry is independent of indent size and thus affords a convenient measure of hardness [3]. It appears from the literature that little study of crack patterns and hardness variations has been made for non-cubic crystals. We have been successful in growing larger and very perfect single crystals of cadmium oxalate trihydrate using a typical nucleation control procedure [4]. The crystals have been characterized by thermal [5], dissolution [6] and electrical properties. It is the purpose of this paper to bring to light the mechanical behaviour and thus make a systematic investigation of the hardness of the gel-grown cadmium oxalate crystals by subjecting three of its prominent as-grown faces, ($\bar{2}\bar{2}1$), (110), (001), and the only cleavage plane, namely ($1\bar{1}0$), to indentation in the laboratory at room temperature ($\sim 27^\circ$ C) and a relative humidity of 41%.

2. Experimental procedure

Grown crystals with smooth surfaces were selected, after examining them under the optical microscope. Microhardness static indentations were made with a pyramid diamond, using Vickers microhardness tester MO 62 70. Loads (P) varying from 5 to 200 g were applied for a fixed interval of time, i.e. 10 sec. In another set of experiments, choosing one particular face of the crystal, a constant load of 50 g was applied for different lengths of time from 2 to 50 sec. Taking 10 indentation trials for each loading, a mean value for the diagonal length was determined and the VHN calculated using the formula:

$$\text{VHN} = 1.854 \times \frac{P}{d^2},$$

where P is the applied load (kg) and d is the diagonal length of the indentation figure (mm).

To our knowledge the structure of cadmium oxalate trihydrate crystals has not been elaborately studied, thus the majority of its grown faces and directions are unindexed. The crystallographic orientation of the diamond indenter with respect to the indenter plane is, therefore, not known. Nevertheless, to avoid possible error due to misorientation in different trials, the indenter orientation was always kept constant by indenting just perpendicular to any particular plane and by translating the plane in steps only in one direction to obtain several indentation marks parallel to one of its edges. This would eliminate any possible error which might, otherwise, have been introduced due to the misorientation during the study of the

0022–2461/82/102825–06$03.22/0

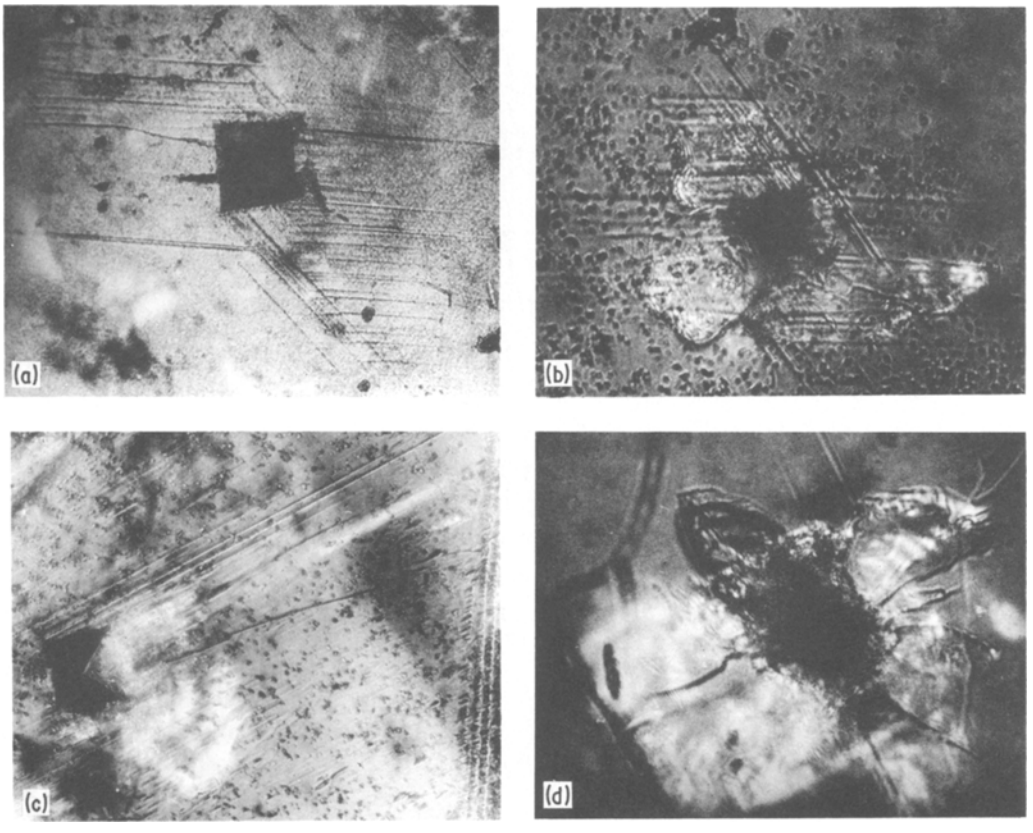

Figure 1 Typical indentation pattern on (a) $(\bar{2}\bar{2}1)$, ×530, (b) (110), ×820, (c) (001), ×440, and (d) $(1\bar{1}0)$, ×770, planes.

effect of load on VHN. The orientation dependence of microhardness, as demonstrated, among others, by Daniels and Dunn [7[and Brasen [8] has been avoided.

The probable error of the mean VHN based on five to 10 indentations for a given plane and environment always lay within 4% of the average value. However, it was sometimes observed that due to slight deviation from the right angle made by the indenter axis and the crystal surface, two of the four vertices of the indentation mark on some of the samples were not well defined, and in such cases measurements of the lengths of diagonals were not very correct. To minimize the error, half diagonals were measured; five or six rows of indentations were made on each surface and the mean diagonal was used for the calculation of VHN. The diagonals were measured using a filar micrometer of the Vickers projection metallurgical microscope. The indented samples were etched in 4 M $CdCl_2$ solution, which is identified as one of the dislocation etches [6, 9], to reveal the surface of the dislocation pattern around indentation marks.

3. Observations and discussion

Considerable cracking around an indentation mark is observed and the typical indentation patterns produced on $(\bar{2}\bar{2}1)$, (110), (001) and $(1\bar{1}0)$ planes are shown in Fig. 1a to d, respectively. All the crack patterns, except those on $(1\bar{1}0)$ planes, are recognized as being composed of slip lines.

Interesting, well-defined slip lines observed (Fig. 1a) on the $(\bar{2}\bar{2}1)$ plane are seen to have formed by a large number of straight cracks or median vents which originate at the sides of the indentation pit. The initiation and propagation of the cracks, according to Dekker and Rieck [10], should depend on the crystallographic situation of glide planes and not on indenter orientation. Mostly the cracks are seen to be parallel to each other, some of them are very long, extending up to 600–700 μm on the crystal surface. The two sets of vents intersect at an angle of nearly 136°. This is also verified by the dense etch traces on the typical $(\bar{2}\bar{2}1)$ face etched in 4 M $CdCl_2$ after indentation, shown in Fig. 2a. It appears that the motion of either set of vents is obstructed by the other. It may be, therefore, that (010) and (001)

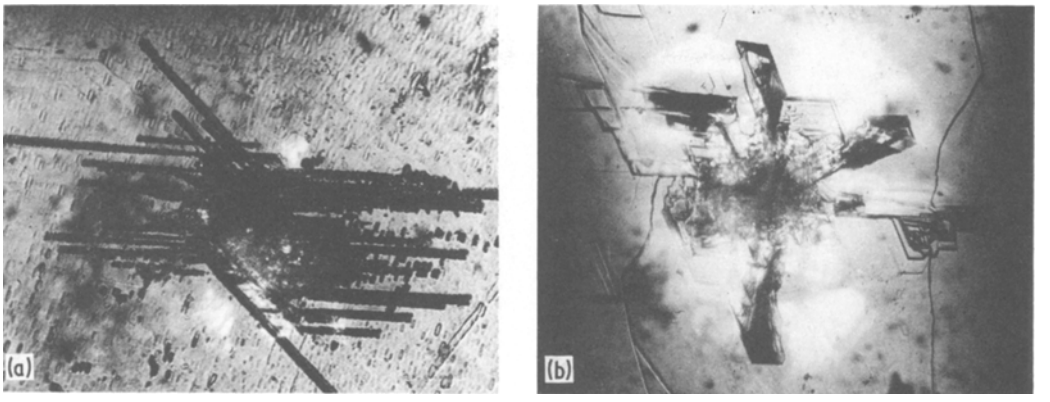

Figure 2 Indentation rosettes revealed on (a) the $(\bar{2}\bar{2}1)$ plane, ×440, and (b) the $(1\bar{1}0)$ plane, ×440, after selective etching in 4 M $CdCl_2$ solution.

planes, known to be meeting at an angle of 135° 52′, represent the operative slip planes in the crystals.

In the case of the cleavage plane, i.e. $(1\bar{1}0)$, some material is seen to be chipped off from around the indentation mark (Fig. 1d) which occurs even with the smallest load applied and the shortest dwell time. The degree of chipping has, however, been found to depend on the load, and the material chips off non-uniformly from different sides of the indentation mark. Crack propagation is not common and the vents are not only of very short length but also spread in random directions, giving the appearance of a "star" crack system as in soda-lime glass [11]. This fact is quite evident from the etched surface shown in Fig. 2b. The authors are inclined to conjecture from Fig. 1d that chipping occurs where median and lateral vent cracks intersect, as is evident from the discharge fragment in transmitted light. Since the lateral vents develop during unloading [11, 12], they must be connected in some way with the residual stresses induced by the inelastic deformation zone. Our understanding of the residual field is very meagre for want of knowledge of events occurring within the zone itself.

The propagation and development of crack patterns on the (1 1 0) plane are of the same nature as those formed on the $(\bar{2}\bar{2}1)$ plane (Fig. 1b).

Propagation of cracks on the (001) plane, shown in Fig. 1c, is of a slightly different nature from that on other planes. A bunch of cracks can be seen shooting out from one edge of the indentation mark, imposing the typical look of a "comet" whose head is the indentation mark itself. It is interesting to note that the crack vents, constituting the bunch of deformation cracks, are not all exactly parallel and linear. Fractures from no other points of the indentation mark are seen. This is contrary to what is observed in the case of the $(\bar{2}\bar{2}1)$ plane. A slight chipping could, however, be observed in the case of high loads.

The mechanism of formation of vents and the chipping off of material may be understood as follows. The sharp point of the pyramid indenter produces an inelastic deformation zone at some threshold, and a deformation-induced flow suddenly develops into a small crack (referred to as median vent) on a plane of symmetry containing the contact axis. Increase in the load changes further the stable growth of a median vent. On unloading, the median vent begins to close, but not heal. In the course of indenter removal, the cracks extending sideways, which are termed lateral vents, begin to develop. After complete removal of the load, the lateral vents continue their extension on the specimen surface and may lead to chipping. Since the cracks have some effective dimension, the model suggested by Lawn and Evans [13] for microfracture beneath the apex of the indenter, seems applicable. Also, as the chipping at all loads is larger in size than the indentations themselves, which is different on different planes, the crystals are likely to exhibit hardness anisotropy.

To better characterize the mechanical properties of the crystals, log load against log diagonal length were established. Figs 3a to c show the variation of the square of the diagonal length, d^2 (mm^2) with load, P (g). Contrary to theoretical prediction, supported by the formula, $VHN = 1.854 \times P/d^2$, it was found that in the case of

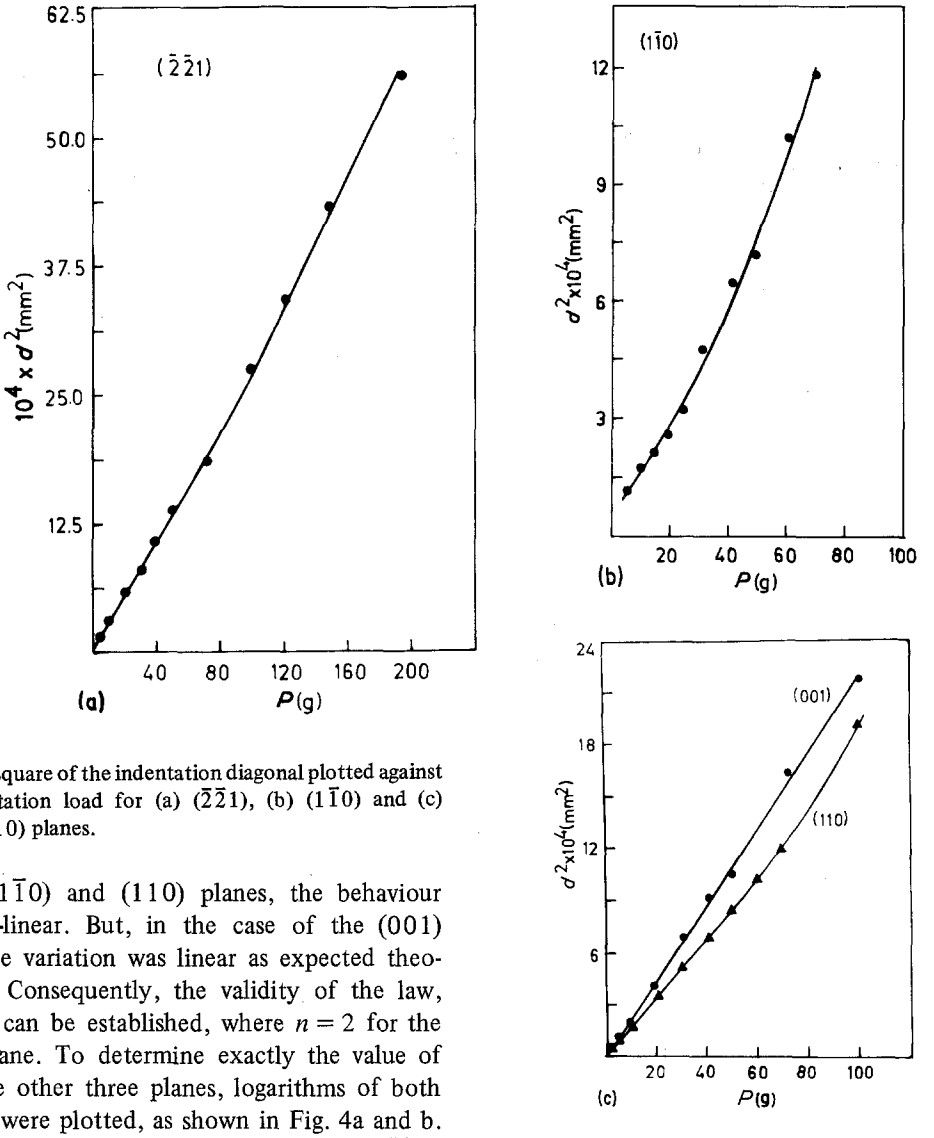

Figure 3 Square of the indentation diagonal plotted against the indentation load for (a) $(\bar{2}\bar{2}1)$, (b) $(1\bar{1}0)$ and (c) (001), (110) planes.

$(\bar{2}\bar{2}1)$, $(1\bar{1}0)$ and (110) planes, the behaviour was non-linear. But, in the case of the (001) plane, the variation was linear as expected theoretically. Consequently, the validity of the law, $P = ad^n$, can be established, where $n = 2$ for the (001) plane. To determine exactly the value of n for the other three planes, logarithms of both P and d were plotted, as shown in Fig. 4a and b. It is seen that the behaviour for the planes $(\bar{2}\bar{2}1)$, (110) and (001) is linear in the entire range of loads and gives slopes of 2.024, 2.018 and 1.886, respectively. However, in a plot of $\log P$ against $\log d$ for the cleavage $(1\bar{1}0)$ plane, two different straight line regions are distinguishable. The slope corresponding to low loads (up to about 30 g) is 3.4, while that corresponding to high loads (between 30 and 200 g) is 2.042. So, except in the case of the initial part of $\log P$ against $\log d$ variation for the $(1\bar{1}0)$ plane, all four planes give values of $n \approx 2$, as theoretically known.

VHN was found to be a function of indenter load and independent of loading or dwell time, implying thereby that unlike other non-metallic materials such as MgO [14–16] the hardness of $Cd(OOC)_2 \cdot 3H_2O$ crystals is not affected by the surface-adsorbed HOH molecules. The anisotropy in hardness observed by indentation on various planes is evident from the graphical plot of VHN (kg mm^{-2}) against applied load P (g), as shown in Fig. 5. It follows from the figure that VHN varies with load in a complex manner, the variation being the sharpest for smaller loads. Variation in hardness with loads less than about 30 g is not uniform, nor follows a systematic path. In the case of (001) and (110) planes, VHN decreases initially up to a load of 30 and 20 g, respectively. On the cleavage plane $(1\bar{1}0)$, on the other hand, VHN increases monotonically up to about 20 g, and then drops rapidly up to about 30 g and extremely slowly thereafter. The $(\bar{2}\bar{2}1)$ plane exhibits a VHN mostly independent of applied load over the entire range, ignoring the small initial rise up to about

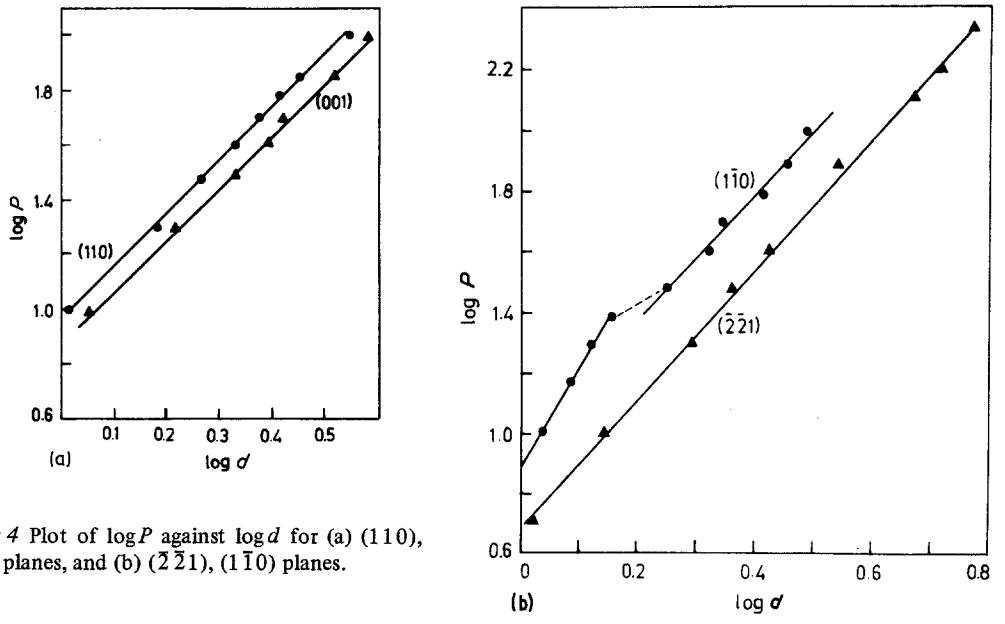

Figure 4 Plot of log$P$ against log$d$ for (a) (110), (001) planes, and (b) ($\bar{2}\bar{2}$1), (1$\bar{1}$0) planes.

12 g. The general impression is that, irrespective of the planes indented, there appears a larger high load (> 30 g) region where VHN is fairly independent of the applied load, although the average load independent hardness value is different for different planes, as given below.

$$VHN_{1\bar{1}0} = 110.0\ kg\ mm^{-2}$$
$$VHN_{100} = 104.5\ kg\ mm^{-2}$$
$$VHN_{001} = 76.0\ kg\ mm^{-2}$$
$$VHN_{\bar{2}\bar{2}1} = 67.0\ kg\ mm^{-2}$$

Obviously, then, $VHN_{1\bar{1}0} > VHN_{100} > VHN_{001} > VHN_{\bar{2}\bar{2}1}$.

The interesting behaviour shown by the curves in Fig. 4 becomes more understandable if we seek an explanation in terms of material chipping and the effect of the distorted zone. During the process of indentation, the indenter penetrates a depth comparable with, or greater than, the thickness of the distorted zone since this zone is pierced by the indenter, and its effect will be marked at relatively low loads. Consequently, a noticeable increase in VHN is observed for (1$\bar{1}$0) and ($\bar{2}\bar{2}$1)

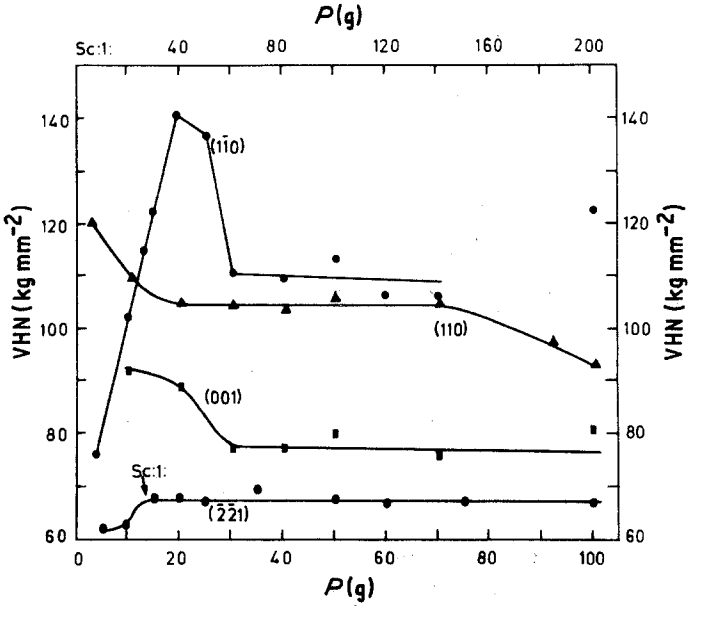

Figure 5 Plot of Vickers microhardness number against indentation load.

planes in the beginning whence the chipping of the material from the surface is very intense. But, in the case of (001) and (110) planes, where the chipping was not so intense, there is a marked decrease in the hardness value. As the depth of the impression of the diamond pyramid increases, the effect of the distorted zone becomes much less prominent, which explains why the variation of VHN with load is almost nil beyond a 30 g load. In fact, for larger loads (above 30 g) the indenter might be reaching a depth at which distorted layers of material exist and the microhardness ceases to be a function of load. For crystals with larger surface energies, therefore, we must apply a large load to prevent the crystal surface from having a substantial effect on the microhardness.

The low microhardness values on the grown faces, compared to those on the cleavage faces, may, however, be attributed to the acute angles formed, as thought by Tsinzerling *et al.* [17]. Because of the lack of knowledge of the crystal structure, a specific explanation for the observed intrinsic anisotropy in the response of cadmium oxalate crystals to the Vickers micro-indentation testing cannot be given at this stage. The amount of anisotropy can, however, be related, as suggested by Armstrong and Raghuram [18], to the possible difference in inclination of the glide planes that accommodate dislocation motion during indentation. The larger the angle of inclination, the larger will be the microhardness, as proposed by Boyarskaya *et al.* [19–21].

4. Conclusions

(1) Slip traces and the chipping of material around indentation figures are observed on the four prominent planes of $CdC_2O_4 \cdot 3H_2O$ single crystals.

(2) The behaviour of pit diagonals against load varies from plane to plane, indicating that the damage done to crystals is stress dependent.

(3) The resulting linear plot of $\log P$ against $\log d$ for the different crystal planes, giving a slope nearer to the theoretical value of 2, indicates that, in the region investigated, the VHN is independent of the applied load.

(4) Large anisotropy in VHN is observed. Although the behaviour is different for the initial smaller values of the applied load, the indentation on all four planes resulted in a region where the VHN is not a function of the applied load.

(5) The microhardness anisotropy may probably result from the possible difference in the angles of intersections of the glide planes with the observation planes.

Acknowledgements

We wish to thank UGC, New Delhi, and CSIR, New Delhi for the sanction of Research Fellowships to T.A.A. and R.S.G., and to G.S.T., respectively.

References

1. H. BUCKLE, *Met. Rev.* **4** (1959) 49.
2. H. BUCKLE, "L'essai de microdurete et ses applications" (Publications Scientifiques et techniques du Ministere de l'Air, Paris, 1960).
3. D. TABOR, "The Hardness of Metals" (Clarendon Press, Oxford, 1951).
4. S. K. ARORA and TOMY ABRAHAM, *Ind. J. Pure Appl. Phys.* **19** (1981) 199.
5. *Idem, J. Crystal Growth* **52** (1981) 851.
6. *Idem, J. Mater. Sci.* **17** (1982).
7. F. W. DANIELS and C. G. DUNN, *Trans. ASM*, **41** (1949) 419.
8. D. BRASEN, *J. Mater. Sci.* **11** (1976) 791.
9. S. K. ARORA and TOMY ABRAHAM, *Crystal Res. Tech.* **17** (1982) 489.
10. E. H. L. J. DEKKER and G. D. RIECK, *J. Mater. Sci.* **9** (1974) 1839.
11. B. R. LAWN and R. WILSHAW, *ibid.* **10** (1975) 1049.
12. E. M. ALMOND and B. ROBUCK, "Scanning Electron Microscopy: Systems and Applications", Conference Proceedings (Institute of Physics, London, 1973).
13. B. R. LAWN and A. E. EVANS, *J. Mater. Sci.* **12** (1977) 2195.
14. J. H. WESTBROOK and P. J. JORGENSEN, *Amer. Mineral.* **53** (1968) 1899.
15. A. R. C. WESTWOOD, D. L. GOLDHEIM and R. G. LYE, *Phil. Mag.* **16** (1967) 505.
16. *Idem, ibid.* **17** (1968) 951.
17. L. G. TSINZERLING, E. S. BERKOVICH, L. A. SYSOEV and M. P. SHASKOL'SKAYA, *Sov. Phys. Crystall.* **14** (1970) 897.
18. R. W. ARMSTRONG and A. C. RAGHURAM, in "The Science of Hardness Testing and its Research Applications", edited by J. Westbrook and H. Conrad (American Society for Metals, Ohio, USA, 1973) Ch. 13.
19. YU. S. BOYARSKAYA and M. I. VAL'KOVSKAYA, in "Sclerometry", (in Russian) (Nauka, Moscow, 1968).
20. YU. S. BOYARSKAYA and D. Z. GRABCO, *Krist. Tech.* **8** (1973) 1367.
21. C. A. BROOKES and R. P. BURNAND, in "The Science of Hardness Testing and its Research Applications", edited by J. Westbrook and H. Conrad (American Society for Metals, Ohio, USA, 1973) Ch. 15.

Received 15 May 1981
and accepted 11 February 1982